# PARAMETRIC ESTIMATION OF MULTI-LINE PARAMETERS BASED ON SLIDE ALGORITHM

*Slobodan Djukanović, Marko Simeunović, Igor Djurović*

Electrical Engineering Department, University of Montenegro, Podgorica, Montenegro
E-mails: {slobdj,markos,igordj}@ac.me, Web: www.tfsa.ac.me

## ABSTRACT

The subspace-based line detection (SLIDE) algorithm enables the estimation of parameters of multiple lines within a digital image by mapping these lines to frequency modulated (FM) signals. In this paper, we consider the estimation of such obtained FM signals by using estimators developed for polynomial-phase signals (PPSs). For this purpose, a recently proposed method that combines the cubic phase function (CPF) and high-order ambiguity function (HAF), referred to as the product CPF-HAF (PCPF-HAF), has been used. Simulations show that the PCPF-HAF-based estimator is more accurate than the estimators based on time-frequency representations.

***Index Terms***— SLIDE, line estimation, polynomial-phase signal, PHAF, PCPF-HAF

## 1. INTRODUCTION

The subspace-based line detection (SLIDE) algorithm has found numerous applications in image and video processing, including the estimation of motion parameters in video-sequences [1–7]. A key step in the SLIDE algorithm is mapping of lines within an image to frequency modulated (FM) signals. This step is performed by using the constant $\mu$-propagation or the variable $\mu$-propagation.

If an image contains straight lines only, the SLIDE produces a sum of sinusoids. Features of these sinusoids can be extracted using some classical spectral estimation tools, such as the periodogram [8] or ESPRIT [9]. However, when lines are not straight, the obtained signal is an FM one, which renders the classical estimation tools non-suitable for the line estimation. The time-frequency (TF) representations have been proposed to deal with FM signals generated by non-straight lines in SLIDE [4]. These FM signals can be approximated by polynomial-phase signals (PPSs). In this paper, we consider the phase/frequency estimation of such obtained PPSs using the combination of the cubic phase function (CPF) and high-order ambiguity function (HAF), referred to as the product CPF-HAF (PCPF-HAF) [10]. In terms of the estimation accuracy, the PCPF-HAF outperforms methods based on the TF representations, as shown in simulations.

The paper is organized as follows. In Section 2, transformation of image containing line patterns to the sum of FM signals with polynomial modulation is demonstrated. In Section 3, we overview the existing PPS estimators such as the product high-order ambiguity function (PHAF) and the CPF [11], as well as the state-of-the-art approach PCPF-HAF [10]. Simulations are given in Section 4. Concluding remarks are given in Section 5.

## 2. SLIDE ALGORITHM

Consider a 2D image with zero-valued background and a line that can be described with parametric coordinates $(x(t), y(t))$:

$$f(x,y) = \delta(x - x(t), y - y(t)), \tag{1}$$

where $\delta(x,y)$ represents the 2D Dirac delta function. In the SLIDE algorithm [1, 2], the image $f(x,y)$ is transformed to two 1D signals:

$$\begin{aligned} f_1(x) &= \int_{-\infty}^{\infty} f(x,y) e^{j\mu_1(x,y)} dy, \\ f_2(y) &= \int_{-\infty}^{\infty} f(x,y) e^{j\mu_2(x,y)} dx, \end{aligned} \tag{2}$$

which are in turn used for the line parameter estimation. Since the propagation functions $\mu_1(x,y)$ and $\mu_2(x,y)$ are real-valued, $f_1(x)$ and $f_2(y)$ are FM signals, which can be analyzed by numerous spectral analysis techniques.

### 2.1. Constant $\mu$-propagation

Consider the straight line case

$$f(x,y) = \delta(y - ax - b), \tag{3}$$

where the line parameters $(a, b)$ are to be estimated. By using the constant $\mu$-propagation, i.e.

$$\mu_1(x,y) = \mu y \qquad (\mu = \text{const}), \tag{4}$$

This work has been supported in part by the Ministry of Science of Montenegro, the FP7 For*e*-Mont project (Grant Agreement No. 315970 FP7-REGPOT-CT-2013) and the BIO-ICT Centre of Excellence (Contract No. 01-1001).

the function $f_1(x)$ becomes a complex sinusoid

$$f_1(x) = \int_{-\infty}^{\infty} \delta(y - ax - b) e^{j\mu y} dy = e^{j\mu(ax+b)}, \qquad (5)$$

whose initial phase and frequency depend on $b$ and $a$, respectively. Numerous methods for the estimation of complex sinusoid exist in the literature (see [12] and references therein). Note also that the parameter $b$ cannot be estimated using this form of propagation due to ambiguity in signal phase.

### 2.2. Variable $\mu$-propagation

The variable $\mu$-propagation [1] is obtained with

$$\mu_1(x, y) = \mu y^2, \qquad (6)$$

which yields a linear FM signal (chirp)

$$f_1(x) = \exp(j\mu(ax + b)^2), \qquad (7)$$

whose parameters can be estimated by several approaches [13, 14].

Consider now an image containing a polynomial line

$$f(x, y) = \delta\left(y - \sum\nolimits_{i=0}^{M} a_i x^i\right). \qquad (8)$$

The variable $\mu$-propagation transforms $f(x, y)$ to

$$\begin{aligned} f_1(x) &= e^{j\mu\left(\sum_{m=0}^{M} a_m x^m\right)^2} \\ &= e^{j\mu \sum_{m=0}^{M} \sum_{n=0}^{M} a_m a_n x^{m+n}} \end{aligned}$$

whose instantaneous frequency (IF)

$$\omega(x) = \mu \sum_{m=0}^{M} \sum_{n=0}^{M} (m + n) a_m a_n x^{m+n-1} \qquad (9)$$

is highly non-stationary for $M > 1$.

Commonly, the TF representations of high order PPSs are characterized by significant inner interferences that cause bias in the IF estimation [15]. In addition, extraction of line parameters from the IF requires solving a set of non-linear equations. Therefore, in order to improve the estimation of polynomial lines, an alternative approach has been proposed in [4] having the following propagating function:

$$\mu_1(x, y) = \mu x y, \qquad (10)$$

which for the polynomial line (8) gives

$$f_1(x) = e^{j\mu \sum_{m=0}^{M} a_m x^{m+1}} \qquad (11)$$

with the IF

$$\omega(x) = \mu \sum_{m=0}^{M} a_m (m + 1) x^m. \qquad (12)$$

As opposed to the $2M - 1$ polynomial order in (9), the IF now has the order of $M$. Reduction of the polynomial order in frequency/phase means that both TF-based and PPS-based estimators will be more accurate. Coefficients of the IF $\omega(x)$ are now directly proportional to that of polynomial line $\{a_i, i = 0, 1, ..., M\}$, whereas in (9) it is cumbersome to establish a relation between the line parameters and signal phase.

## 3. ESTIMATION METHODS

The multi-lag high-order instantaneous moment (ml-HIM) of a discrete signal $x(n), n = 0, \cdots, N - 1$, is defined as [16]

$$\begin{aligned} x_1(n) &= x(n), \\ x_2(n; \boldsymbol{\tau}_1) &= x_1(n) x_1^*(n + \tau_1), \\ x_3(n; \boldsymbol{\tau}_2) &= x_2(n; \boldsymbol{\tau}_1) x_2^*(n + \tau_2; \boldsymbol{\tau}_1), \\ &\cdots \\ x_P(n; \boldsymbol{\tau}_{P-1}) &= x_{P-1}(n; \boldsymbol{\tau}_{P-2}) x_{P-1}^*(n + \tau_{P-1}; \boldsymbol{\tau}_{P-2}), \end{aligned} \qquad (13)$$

where $\boldsymbol{\tau}_i = [\tau_1, \tau_2, \cdots, \tau_i]$, $i = 1, ..., P - 1$, are the sets of time lags. The multi-lag HAF (ml-HAF) is defined as the discrete Fourier transform (DFT) of the ml-HIM [16],

$$X_P(f; \boldsymbol{\tau}_{P-1}) = \sum_{n=0}^{N-1} x_P(n; \boldsymbol{\tau}_{P-1}) e^{-j2\pi f n}. \qquad (14)$$

If $x(n)$ is a monocomponent $P$th order PPS, i.e.

$$x(n) = A e^{j2\pi \sum_{m=0}^{P} a_m (n\Delta)^m},$$

where $a_m$ are the polynomial coefficients and $\Delta$ is the sampling interval, the $P$th order ml-HIM of $x(n)$ is a complex sinusoid with frequency $f = \Delta^P P! a_P \prod_{k=1}^{P-1} \tau_k$. By estimating this frequency [12], we can also estimate $a_P$. Lower order coefficients are obtained by repeating the same procedure on the signal $x(n)$ dechirped by the previously estimated higher order coefficients [14, Section III].

When $x(n)$ is a mc-PPS, i.e.

$$x(n) = \sum_{k=1}^{K} A_k e^{j2\pi \sum_{m=0}^{P} a_{k,m} (n\Delta)^m},$$

where $a_{k,m}$ are the coefficients of the $k$th component, the $P$th order ml-HIM will contain $K$ complex sinusoids corresponding to the auto-terms. In addition to the auto-terms, the ml-HIM will contain a large number of cross-terms which are, in general, $P$th order PPSs [16].

### 3.1. PHAF

The cross-terms can be significantly attenuated using the PHAF [16]. First, $Q$ sets of time lags are introduced as follows:

$$\mathbf{T}_{P-1}^{Q} = \left[\boldsymbol{\tau}_{P-1}^{(1)}, \boldsymbol{\tau}_{P-1}^{(2)}, \cdots, \boldsymbol{\tau}_{P-1}^{(Q)}\right],$$

where $\boldsymbol{\tau}_{P-1}^{(q)} = \left[\tau_1^{(q)}, \tau_2^{(q)}, \cdots, \tau_{P-1}^{(q)}\right]$ and $q = 1, ..., Q$. The PHAF is then defined as

$$X_P^Q(f, \mathbf{T}_{P-1}^Q) = \prod_{q=1}^{Q} X_P(\beta^{(q)} f, \boldsymbol{\tau}_{P-1}^{(q)}), \tag{15}$$

where $\beta^{(q)} = \prod_{k=1}^{P-1} \tau_k^{(q)}/\tau_k^{(1)}$ represents the frequency scaling coefficient. The PHAF exploits the fact that the frequencies of auto-terms are proportional to the product of time lags, which is not the case for the frequencies of cross-terms. Therefore, after scaling in frequency by $\beta^{(q)}$, the auto-terms will align in frequency, whereas the cross-terms will not. Consequently, a product of several ml-HAFs (15) will result in suppressing the cross-terms with respect to the auto-terms.

Coefficients of multiple PPSs can be efficiently estimated using an iterative PHAF-based method proposed in [17]. With calculation of only several additional PHAF points, the auto-term frequency can be estimated very accurately, thus preventing the need for oversampling the PHAF domain, which represents the straightforward approach.

### 3.2. CPF, CPF-HAF and PCPF-HAF

Each auto-correlation in (13) increases the signal-to-noise (SNR) threshold by approximately 6 dB [18] and produces additional interference terms. Reducing the number of PDs, therefore, will improve the accuracy of technique that uses the auto-correlations (13) as the means of parameter estimation. The transform that exploits this fact is the CPF proposed in [11] for the estimation of cubic phase signals ($P = 3$). The CPF is defined as

$$\mathrm{CPF}_x(n, \Omega) = \sum_k x(n+k)x(n-k)e^{-j\Omega(k\Delta)^2}. \tag{16}$$

Parameters $a_3$ and $a_2$ can be estimated from the CPF evaluated at two instants, say $n = 0$ and $n = n_1$, as

$$\hat{a}_2 = \hat{\Omega}_0/(2a_2), \quad \hat{a}_3 = (\hat{\Omega}_{n_1} - \hat{\Omega}_0)/(6n_1\Delta a_3),$$
$$\hat{\Omega}_{0/n_1} = \arg\max_{\Omega} |\mathrm{CPF}_x(0/n_1, \Omega)|^2. \tag{17}$$

Since for a cubic phase signal only one auto-correlation is calculated, as opposed to two in the HAF, the CPF outperforms the HAF in terms of accuracy and SNR threshold.

In [10], a method for parameter estimation of PPSs of order more than three is proposed. The method combines the CPF and the HAF, and is referred to as the CPF-HAF. It provides more robust and more accurate results than the standard HAF/PHAF-based approaches. The CPF-HAF starts from the fact that the ml-HIM $x_{P-2}(n; \boldsymbol{\tau}_{P-3})$ of a $P$th order PPS $x(n)$ is a third-order PPS with coefficients $a_2$ and $a_3$ proportional to coefficients $a_{P-1}$ and $a_P$, respectively, of $x(n)$. Therefore, the CPF-HAF is defined as the CPF of $x_{P-2}(n; \boldsymbol{\tau}_{P-3})$, i.e.

$$\mathrm{CPF\text{-}HAF}_x(n, \Omega) = \sum_k x_{P-2}(n+k; \boldsymbol{\tau}_{P-3}) x_{P-2}(n-k; \boldsymbol{\tau}_{P-3}) e^{-j\Omega(k\Delta)^2}. \tag{18}$$

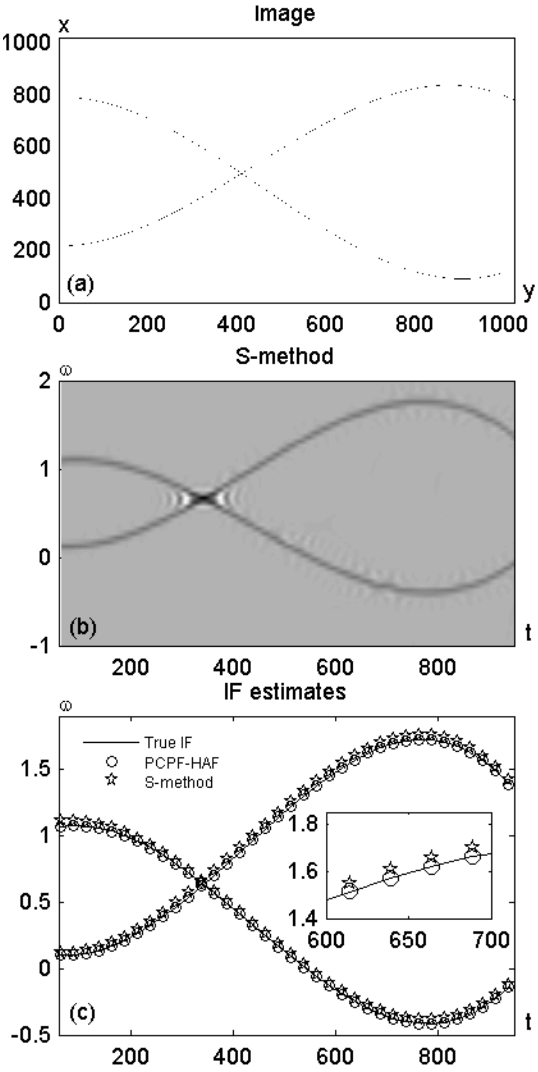


**Fig. 1**. (a) Image. (b) S-method of FM signals obtained by SLIDE. (c) IF estimations by the S-method and the PCPF-HAF.

Following the same rationale as in the PHAF case, the product version of the CPF-HAF is defined as

$$\mathrm{PCPF\text{-}HAF}_x(n, \Omega) = \prod_{q=1}^{Q} \mathrm{CPF\text{-}HAF}_x^q(n, \beta^{(q)}\Omega), \tag{19}$$

where $\mathrm{CPF\text{-}HAF}_x^q$ is the CPF-HAF calculated with the lag set $\boldsymbol{\tau}^{(q)}$, $Q$ is the number of different lag sets and $\beta^{(q)} = \prod_{i=1}^{P-3} \tau_i^{(q)}/\tau_i^{(1)}$ is the scaling operator in the $\Omega$ domain.

## 4. SIMULATIONS

**Example 1:** Here, we will compare the performances of the PCPF-HAF and the S-method [4] in estimating coefficients of polynomial lines within an image. To that end, consider the

**Table 1**. Estimated polynomial-line parameters

| | S-method | PCPF-HAF |
|---|---|---|
| $a_{1,3}$ | $-1.941 \cdot 10^{-6}$ | $-1.95 \cdot 10^{-6}$ |
| $a_{1,2}$ | $3.275 \cdot 10^{-3}$ | $3.302 \cdot 10^{-3}$ |
| $a_{1,1}$ | $-0.659$ | $-0.689$ |
| $a_{1,0}$ | $143.16$ | $128.93$ |
| $a_{2,3}$ | $1.784 \cdot 10^{-6}$ | $1.857 \cdot 10^{-6}$ |
| $a_{2,2}$ | $-3.09 \cdot 10^{-3}$ | $-3.257 \cdot 10^{-3}$ |
| $a_{2,1}$ | $0.712$ | $0.836$ |
| $a_{2,0}$ | $834.17$ | $781.62$ |

image containing two cubic curves as follows:

$$f(x,y) = \delta(y - a_{1,3}x^3 - a_{1,2}x^2 - a_{1,1}x - a_{1,0}) + \delta(y - a_{2,3}x^3 - a_{2,2}x^2 - a_{2,1}x - a_{2,0}), \tag{20}$$

where $a_{1,3} = -1.948 \cdot 10^{-6}$, $a_{1,2} = 3.306 \cdot 10^{-3}$, $a_{1,1} = -0.697$, $a_{1,0} = 130$, and $a_{2,3} = 1.855 \cdot 10^{-6}$, $a_{2,2} = -3.26 \cdot 10^{-3}$, $a_{2,1} = 0.843$, $a_{2,0} = 780$, which is shown in Fig. 1a. The image size is $1024 \times 1024$. The modified variable $\mu$-propagation (10) is performed with $\mu = 0.00125$[1]. The PCPF-HAF is calculated following the guidelines given in [10]. The S-method of the signal (11) is represented in Fig. 1b. The estimations of coefficients $a_{k,i}$, $k = 1, 2$ and $i = 0, 1, 2, 3$, are presented in Table 1. Clearly, the S-method is outperformed by the PCPF-HAF in terms of accuracy.

The IF estimations obtained using the PCPF-HAF method (circles) and the S-method (pentagrams) are given in Fig. 1c. A small region in Fig. 1c is zoomed in to emphasize the difference between the techniques. The IF estimation obtained using the S-method is biased, as expected. On the other hand, the IF estimations based on the PCPF-HAF follow the true IF values completely.

Since the PHAF performs similarly to the PCPF-HAF, we have not presented the PHAF-based results.

**Example 2:** In this example, we compare the S-method and the PCPF-HAF in estimating polynomial coefficients of a single cubic curve corrupted by Gaussian noise $\nu(x)$ of standard deviation $\sigma$, i.e.

$$f(x,y) = \delta(y - a_3x^3 - a_2x^2 - a_1x - a_0 + \nu(x)). \tag{21}$$

Curve coefficients $a_3$, $a_2$, $a_1$ and $a_0$ are equal to $a_{1,3}$, $a_{1,2}$, $a_{1,1}$ and $a_{1,0}$, respectively, from Example 1. Performance has been evaluated through the mean squared error (MSE) defined as

$$\text{MSE} = 10\log_{10}\left[\frac{1}{N_{MC}}\sum_{k=1}^{N_{MC}}\left(a_{true} - a_{est}^k\right)^2\right], \tag{22}$$

[1]The parameter $\mu$ determines the maximal object velocity in image that can be estimated [3] and its choice depends on particular application.

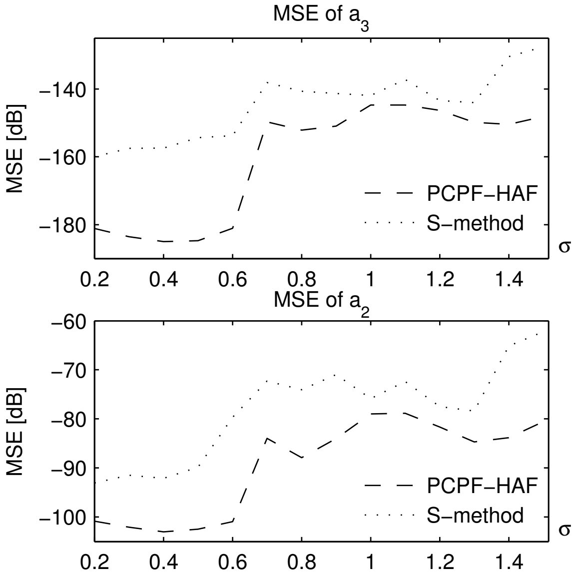


**Fig. 2**. MSE versus noise deviation $\sigma$.

where $a_{true}$ represents the true coefficient value, $a_{est}^k$ the estimated value in the $k$th simulation, and $N_{MC}$ is the number of Monte-Carlo simulations. Here, $N_{MC} = 500$. The MSE of the highest two coefficients $a_3$ and $a_2$ is given in Fig. 2, where $\sigma$ is varied from 0.2 to 1.5 in steps of 0.1. The same PCPF-HAF setup as in Example 1 is used, as well as the same $\mu$. Again, the PCPF-HAF provides more accurate estimates than the S-method.

## 5. CONCLUSIONS

The estimation of multiple lines in image using the SLIDE algorithm is considered. The line parameters are mapped into the IF of FM signals, whose parameters are, in turn, estimated using the recently proposed PCPF-HAF method. Simulations show that the proposed estimator outperforms those based on TF representations, namely the S-method. Also, the proposed method works well even if the line to be estimated is corrupted by Gaussian noise.

## REFERENCES


[1] H.K. Aghajan and T. Kailath, "SLIDE: subspace-based line detection," *IEEE Transactions on Pattern Analysis and Machine Intelligence*, vol. 16, no. 11, pp. 1057–1073, 1994.

[2] H.K. Aghajan, B.H. Khalaj, and T. Kailath, "Estimation of multiple 2-D uniform motions by SLIDE: subspace-based line detection," *IEEE Transactions on Image Processing*, vol. 8, no. 4, pp. 517–526, 1999.

[3] S. Stanković and I. Djurović, "Motion parameter esti-

mation by using time-frequency representations," *Electronics Letters*, vol. 37, no. 24, pp. 1446–1448, 2001.

[4] I. Djurović, S. Stanković, A. Ohsumi, and H. Ijima, "Estimation of line parameters using SLIDE algorithm and TF representations," in *9th International Conference on Electronics, Circuits and Systems*. IEEE, 2002, vol. 3, pp. 1067–1070.

[5] D.S. Alexiadis and G.D. Sergiadis, "Estimation of multiple accelerated motions using chirp-fourier transform and clustering," *IEEE Transactions on Image Processing*, vol. 16, no. 1, pp. 142–152, 2007.

[6] A. Briassouli and N. Ahuja, *Estimation of multiple periodic motions from video*, Springer, 2006.

[7] A. Briassouli, D. Matsiki, and I. Kompatsiaris, "Continuous wavelet transform for time-varying motion extraction," *IET image processing*, vol. 4, no. 4, pp. 271–282, 2010.

[8] P. Stoica and R.L. Moses, *Introduction to spectral analysis*, vol. 1, Prentice Hall New Jersey, 1997.

[9] R. Roy, A. Paulraj, and T. Kailath, "ESPRIT–a subspace rotation approach to estimation of parameters of cisoids in noise," *IEEE Transactions on Acoustics, Speech and Signal Processing*, vol. 34, no. 5, pp. 1340–1342, 1986.

[10] I. Djurović, M. Simeunović, S. Djukanović, and P. Wang, "A hybrid CPF-HAF estimation of polynomial-phase signals: Detailed statistical analysis," *IEEE Transactions on Signal Processing*, vol. 60, no. 10, pp. 5010–5023, 2012.

[11] P. O'Shea, "A fast algorithm for estimating the parameters of a quadratic FM signal," *IEEE Transactions on Signal Processing*, vol. 52, no. 2, pp. 385–393, February 2004.

[12] E. Aboutanios and B. Mulgrew, "Iterative frequency estimation by interpolation on Fourier coefficients," *IEEE Transactions on Signal Processing*, vol. 53, no. 4, pp. 1237–1242, April 2005.

[13] P.M. Djurić and S.M. Kay, "Parameter estimation of chirp signals," *IEEE Transactions on Acoustics, Speech and Signal Processing*, vol. 38, no. 12, pp. 2118–2126, 1990.

[14] S. Peleg and B. Friedlander, "The discrete polynomial-phase transform," *IEEE Transactions on Signal Processing*, vol. 43, no. 8, pp. 1901–1914, August 1995.

[15] Lj. Stanković, "L-class of time-frequency distributions," *IEEE Signal Processing Letters*, vol. 3, no. 1, pp. 22–25, 1996.

[16] S. Barbarossa, A. Scaglione, and G.B. Giannakis, "Product high-order ambiguity function for multicomponent polynomial phase signal modeling," *IEEE Transactions on Signal Processing*, vol. 46, no. 3, pp. 691–708, March 1998.

[17] S. Djukanović and V. Popović, "An efficient peak frequency estimator for product high-order ambiguity function," in *IEEE International Conference on Acoustics, Speech and Signal Processing (ICASSP)*, 2011, pp. 3804–3807.

[18] B. Porat and B. Friedlander, "Asymptotic statistical analysis of the high-order ambiguity function for parameter estimation of polynomial-phase signals," *IEEE Transactions on Information Theory*, vol. 42, no. 3, pp. 995–1001, May 1996.